Determination of the critical value of x_c for the direct-to-indirect band-gap transition in $Al_xGa_{1-x}As$ by measuring hot-carrier dynamics in the X valley

W. B. Wang and R. R. Alfano
Physics Departrment, Institute for Ultrafast Spectroscopy and Lasers, The City College and Graduate School of City University of New York, New York, New York 10031

D. Szmyd and A. J. Nozik
Solar Energy Research Institute, Golden, Colorado 80401
(Received 22 July 1992)

The time evolution of the population of hot electrons in the satellite X valley in $Al_xGa_{1-x}As$ was measured by femtosecond pump-probe infrared (IR)-absorption spectroscopy. The dynamics of the X-valley electrons for samples with $x \leq 0.408$ was found to be different from that for samples with $x \geq 0.439$ which reflects their different types of band gaps. The critical value of x_c that corresponds to the direct-to-indirect band-gap transition for $Al_xGa_{1-x}As$ was determined to be 0.412 ± 0.009 from the composition dependence of the induced IR absorption.

The $Al_xGa_{1-x}As$ alloy system is important for several photonic devices (lasers, light-emitting diodes, and photovoltaic converters) as well as high-speed electronic devices (high-electron-mobility transistors and resonant tunneling diodes).[1] The design of these advanced devices relies on accurate knowledge of the energy band structure of $Al_xGa_{1-x}As$ as a function of x, in particular, on the critical value x_c that corresponds to the direct-to-indirect band-gap transition.[2] However, the values of x_c determined from recent fluorescence and other measurements[2-6] span a large range of 0.37–0.45. One could not design and construct high-quality $Al_xGa_{1-x}As$ devices with such an uncertainty in x_c. Therefore, the precise determination of an accurate value of x_c remains very important for semiconductor physics and device design. Since the probability for indirect transitions is several orders of magnitude smaller than that for direct transitions, the intensity of fluorescence from the satellite valley is much weaker than that from the central valley. Therefore, it is difficult to monitor small changes of the electron distribution among different valleys with x, and to accurately determine x_c by measuring fluorescence from $Al_xGa_{1-x}As$.[1]

In this paper, we present time-resolved infrared (IR) absorption measurements for $Al_xGa_{1-x}As$, and an approach to determine the accurate value of x_c. The measured change of the photoinduced IR absorption monitors the change of the numbers of electrons in the X valley which increases significantly when x approaches x_c. The profile of the measured IR absorption enables us to distinguish between direct and indirect band-gap structures for samples. The values of $\alpha = \Delta(E_g)^{\Gamma}/\Delta x = 13.40$ meV/% and $x_c = 0.412 \pm 0.009$ were determined with a high degree of accuracy from the measured x dependence of the short decay component of the IR absorption.

Five undoped 2-μm-thick $Al_xGa_{1-x}As$ epilayer samples used in our measurements were grown by the metal-organic-chemical-vapor-deposition process in a vertical reactor at a temperature of 725 °C with a growth rate of 12–14 Å/s. The Al contents of the samples were determined by electron microprobe analysis and gas-phase composition measurements in the growth reactor to be 0.358, 0.380, 0.408, 0.439, and 0.595, respectively, with an uncertainty of ± 0.005. The GaAs substrate for each sample was completely removed to eliminate excitation and absorption from the substrate. The steady-state IR transmission spectrum of each sample was measured and found to have no appreciable absorption at the IR probe wavelengths.

The details of the femtosecond visible-pump and IR-probe setup have been reported elsewhere.[7,8] In this measurement, a 585-nm, ~400-fs pulse, obtained from the output of a synchronously pumped Spectral Physics dye laser with a pulse-dye amplifier, was used to pump samples to create hot electrons and holes, and a 3.3-μm, ~500-fs IR-probe pulse, generated in a $LiIO_3$ crystal by the seeded optical parametric method, was used to monitor the photoinduced IR absorption.

The measured growth and decay of the photoinduced IR absorption as a function of x and delay time t_d between pump and probe pulses for the $Al_xGa_{1-x}As$ samples at room temperature are displayed in Fig. 1. The salient features of the curves are the following: the decay of the induced total absorption for samples with $x \geq 0.439$ is flat within the experimental time range of ~45 ps; however, the decay for samples with $x \leq 0.408$ has both short and long flat components. At the peak position of each curve, the percentage of optical density (OD) for the short decay portion in the induced total absorption decreases with increasing x for $x \leq 0.408$ samples, and goes to zero for $x \geq 0.439$ samples.

An explanation for the induced total IR absorption has been previously discussed.[7,9] The induced total IR absorption is attributed to interconduction band absorption (ICA) by electrons from the X_6 to the X_7 valleys; free-carrier absorption (FCA) by holes in the valence bands

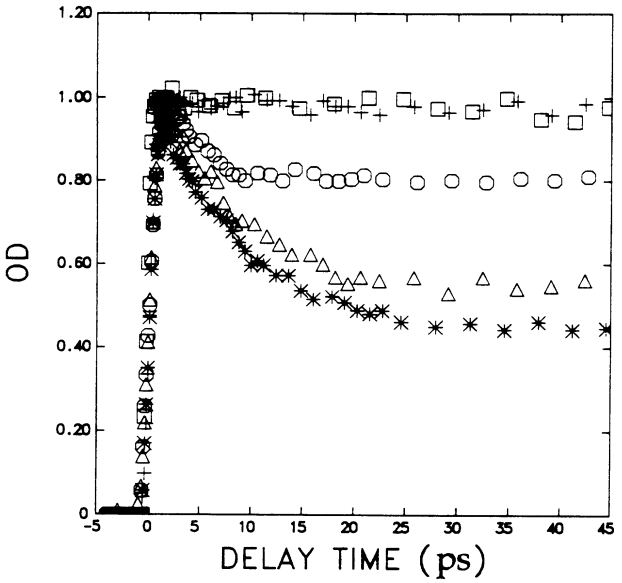

FIG. 1. The measured change in induced (OD) vs delay time at $\lambda_{PROBE}=3.3$ μm for $Al_xGa_{1-x}As$ with $x=0.358$ (stars), 0.380 (triangles), 0.408 (circles), 0.439 (pluses), and 0.595 (squares). In order to clearly show their decay behavior, the maximum value of each curve has been normalized to unity.

and by electrons in the conduction-band valleys; and intervalence band absorption (IVA) by electrons from the split off to the heavy- and light-hole bands and from the light-hole to the heavy-hole bands. Since the calculated values of OD for IVA (Ref. 7) at $\lambda \geq 3.3$ μm are much smaller than the observed values of OD for the corresponding samples, IVA can be neglected in our considerations.

The decay of FCA is flat because the radiative and Auger recombination time of electrons and holes in $Al_xGa_{1-x}As$ is at least several nanoseconds[1] which is much longer than our experimental time scale. The flat decay of FCA has been previously observed in our measurements for GaAs at a long-probe wavelength of 3.9 μm (Ref. 9) in which only FCA is possible because the probe photon of 3.9 μm has insufficient energy to make the $X_6 \rightarrow X_7$ transition.

The temporal characteristics of the $X_6 \rightarrow X_7$ ICA in $Al_xGa_{1-x}As$ depends on its band structure. A sample with $x < x_c$, has a GaAs-like direct band gap. Electrons pumped by a 585-nm photon obtain sufficient energy to undergo intervalley scattering from the Γ valley to the L and X valleys.[10] The population of electrons at the bottom of the X valley, N_X, rapidly increases at first to its maximum. Since the minimum of the X valley is much higher than that of the Γ and L valleys, electrons stay in the X valley for only a short time, and then decay back to the Γ and L valleys. Therefore, N_X and the $X_6 \rightarrow X_7$ ICA as a function of t_d should have a short decay as shown by the curve of $x=0.358$ in Fig. 1.

A sample with $x > x_c$ has an AlAs-like indirect band gap. If pump photons have sufficient energy to excite electrons to reach the X, L, and Γ valleys, electrons will undergo intervalley and intravalley scattering. Since the X minimum is lower than the Γ and L minima, almost all of the electrons will finally scatter into the X valley and stay at its bottom until they recombine with holes in a few hundred nanoseconds.[1] Therefore, the decay of the $X_6 \rightarrow X_7$ ICA should be flat as observed for the sample with $x=0.595$ shown in Fig. 1

In order to understand the change of the short decay portion of the IR-absorption profile with x, the case for $x \approx x_c$ in which the decay of ICA becomes complex should be analyzed. When x increases to almost x_c, the minimum of the X valley is slightly higher than that for the Γ valley. When final thermal equilibrium among the electrons in the Γ, L, and X valleys is obtained, not all of the electrons will be in the Γ valley but some of them will occupy the L and X valleys as schematically shown in Fig. 2(a). In other words, not all of the X valley electrons initially scattered from the Γ and L valleys will decay back to the latter two valleys, but some of them will stay in the X valley for a long time, which will result in the $X_6 \rightarrow X_7$ ICA having a long flat decay. For this type of direct band-gap samples, the $X_6 \rightarrow X_7$ ICA would have both short and flat decay components as shown in Fig. 2(b). When the energy difference between the X and Γ minima, $\Delta E=(E_g)^X-(E_g)^\Gamma$, decreases, the number of electrons in the X valley relative to the total number of electrons in thermal equilibrium will increase, and as a result, the flat decay portion of ICA will become larger, and the short decay portion of the ICA will decrease. Consequently, the measured percentage of the short decay portion of ICA relative to the total absorption, defined as a parameter $K_{short}=(OD)_{short}/(OD)_{total}$, directly reflects the value of ΔE for a sample. The critical value of x_c for which $\Delta E=0$ can be obtained from the measured x dependence of ΔE.

These ideas can be expressed in a mathematical form. The parameter K_{short} can be written as

$$K_{short}=(ICA)_{short}/[(ICA)_{total}+(FCA)_{total}] , \quad (1)$$

where $(FCA)_{total}$, $(ICA)_{total}=(ICA)_{short}+(ICA)_{flat}$, and $(ICA)_{short}$, indicated in Fig. 2(b), correspond to the total absorption for FCA and ICA, and the short decay component of ICA at the absorption peak, respectively.

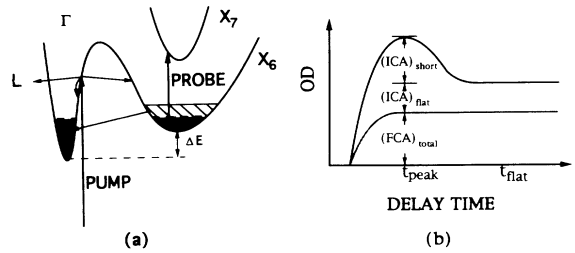

FIG. 2. Schematic diagram indicating (a) band structure involving the Γ and X valleys in $Al_xGa_{1-x}As$ for x slightly smaller than x_c showing ΔE, $(N_X)_{peak}$ (diagonal solid lines), and $(N_X)_{flat}$ (shaded area with diagonal dashed lines) as defined in the text; and (b) a corresponding temporal profile of the induced IR absorption showing $(ICA)_{short}$, $(ICA)_{flat}$, and $(FCA)_{total}$ as described in the text.

The $(FCA)_{total}$ and $(ICA)_{total}$ are given by $(FCA)_{total}=\sigma_{FC}N$ and $(ICA)_{total}=\sigma_{IC}p_XN$, where σ_{FC} and σ_{IC} are cross sections for FCA and ICA, respectively; N is the total carrier density; and p_X is the fraction of the carrier density in the X valley relative to the total carrier density at the delay time corresponding to the absorption peak t_{peak} [see Fig. 2(b)].

The flat decay component of ICA is given by $(ICA)_{flat}=\sigma_{IC}f_XN$, where f_X is the fraction of carrier density in the X valley relative to the total carrier density at the delay time corresponding to the flat absorption region t_{flat} [see Fig. 2(b)]. The short decay component of ICA can be written as $(ICA)_{short}=(ICA)_{total}-(ICA)_{flat}=\sigma_{IC}N[p_X-f_X]$.

Substituting the expressions for $(ICA)_{short}$, $(ICA)_{total}$, and $(FCA)_{total}$ into Eq. (1), K_{short} becomes

$$K_{short}=[1/(\sigma_{FC}/\sigma_{IC}+p_X)][p_X-f_X]\ . \tag{2}$$

The expression for $p_X(x)$ can be written as[11]

$$p_X(x)=[1/t_{\Gamma X}(x)]/[1/t_{\Gamma X}(x)+1/t_{\Gamma L}(x)+1/t_{\Gamma\Gamma}(x)]\ , \tag{3}$$

where $t_{\Gamma X}(x)$, $t_{\Gamma L}(x)$, and $t_{\Gamma\Gamma}(x)$ are intervalley and intravalley scattering times, and vary with Al content x and the experimental conditions such as crystal temperature, kinetic energy of electrons, and so on.

The intervalley and intravalley scattering times for GaAs were previously measured to be $t_{\Gamma X}=55\pm11$ fs for electrons with kinetic energy centered at 0.51 eV,[11] $t_{\Gamma L}=100\pm20$ fs for 0.5-eV electrons,[12] and $t_{\Gamma\Gamma}=165\pm20$ fs for the central valley electrons relaxed from the kinetic energy of 0.61 eV.[13] These measured results can be normalized, using the theory of Conwell and Vassel,[14] to obtain corresponding values of those parameters for GaAs in our experimental conditions.

The x dependence of the scattering rates arises from the x dependence of the effective masses, the deformation potentials, and the alloy-disorder-assisted intervalley scattering rates. The x dependence of the effective masses of $m_\Gamma=0.067+0.083x$, $m_L=0.56+0.1x$, and $m_X=0.85-0.14x$ are given in the literature.[10] The calculations by Cardona and co-workers[15] have shown that the deformation potentials D_{ij} $(i,j=\Gamma,L,X)$ for $Al_xGa_{1-x}As$ changes slightly with x, and can therefore be approximately treated as a linear function of x. The x dependence of alloy-disorder-assisted intervalley scattering (zero-phonon transition) rates can be estimated from the recently measured results of Kalt *et al.*[16] which have shown that (1) alloy-disorder-assisted intervalley scatterings can be negligible for GaAs and $Al_xGa_{1-x}As$ samples with small values of x, but are efficient for $Al_xGa_{1-x}As$ samples with large values of x, (2) in $Al_{0.38}Ga_{0.62}As$, the zero-phonon-assisted intervalley scattering time t_{dis} is about four times longer than that for phonon-assisted transfer, and (3) the effect of the disorder scattering for higher x values can be estimated using the simplified formula $1/t_{dis}\alpha x(1-x)$. The expressions for the x dependence of the effective mass, the deformation potentials, and the alloy-disorder intervalley scattering rates enable us to obtain the x dependence of the scattering rates and to calculate $p_X(x)$ as a function of x.

Since both intravalley and intervalley scattering occur on a time scale which is much shorter than the recombination time of electrons and holes,[11–13,17] electrons in the conduction bands at t_{flat} may be assumed to be in thermal equilibrium and characterized by a Boltzmann distribution. Therefore, $f_X(x)$ can be written as[3]

$$f_X(x)=1/\left[1+\left[\frac{t_X}{t_\Gamma}\right]\left[\frac{m_\Gamma}{m_X}\right]^{3/2}e^{\Delta E_{X\Gamma}/K_BT}+\left[\frac{t_X}{t_L}\right]\left[\frac{m_L}{m_X}\right]^{3/2}e^{\Delta E_{XL}/K_BT}\right]\ , \tag{4}$$

where t_i and m_i are the lifetime and density-of-states effective mass of electrons in the ith valley, respectively, where $i=\Gamma$, L, and X; K_B is the Boltzmann constant; $\Delta E_{X\Gamma}=(E_g)^X-(E_g)^\Gamma$; and $\Delta E_{XL}=(E_g)^X-(E_g)^L$. The previous band-gap determinations suggest a linear dependence[2,10] of $(E_g)^\Gamma(x)$ for $x<x_c$ by $(E_g)^\Gamma(x)=1.424+\alpha x$. Since the value of $(E_g)^\Gamma(x)$ varies greatly[10] from 1.424 eV for GaAs $(x=0)$ to 3.018 eV for AlAs $(x=1)$, and the previously determined values of α scatter in the large range from 12.50 meV/% (Ref. 4) to 16.1 meV/%,[18] α has to be kept as an unknown parameter to be determined. The value of $(E_g)^X$ changes slightly from 1.90 eV for GaAs to 2.168 eV for AlAs, and the difference of its calculated values using different determined expressions of $(E_g)^X$ is small.[10] Therefore, we chose the most used expression[19] of $(E_g)^X(x)=1.90+0.125x+0.143x^2$ for $(E_g)^X(x)$. For a similar reason, we chose[19] $(E_g)^L(x)=1.704+0.642x$ for $(E_g)^L(x)$. Substituting the expressions of $t_i(x)$, $m_i(x)$, $(E_g)^i(x)$ $(i=\Gamma,L,\text{and }X)$ into Eq. (4), $f_X(x)$ was obtained with one unknown parameter α.

The ratio of σ_{FC}/σ_{IC} was found to be 0.418 from Eq. (2) using the calculated values of p_X and f_X, and the measured value of $K_{short}=0.56$ for GaAs $(x=0)$. Substituting the expressions of $p_X(x)$ and $f_X(x)$, and the value of σ_{FC}/σ_{IC} into Eq. (2) shows K_{short} to be a complex function of x with an unknown parameter α.

The measured values of $K_{short}(x)$ for a series of $Al_xGa_{1-x}As$ and GaAs samples are displayed in Fig. 3. The change of $K_{short}(x)$ from 0.56 for $x=0$ to 0.0 for $x=0.439$ mainly arises from $f_X(x)$ because the calculated corresponding values of $p_X(x)$ change less than 4%. In order to fit the calculated values of $K_{short}(x)$ from Eq. (2) to their experimental values, α was treated as a variable parameter. The least-squares fit was used and the best fit, which is shown in Fig. 3, yields a value of $\alpha=13.40$ meV/%. The critical value of x_c was then determined to be 0.412 by solving the equation of $(E_g)^X(x_c)=(E_g)^\Gamma(x_c)$.

Since the number of electrons in the X_6 valley, in thermal equilibrium, relative to the total number of electrons increases significantly when x approaches x_c (i.e., $\Delta E\rightarrow0$), the change in $(ICA)_{short}$ is extremely sensitive to the change in ΔE, and consequently to the determination

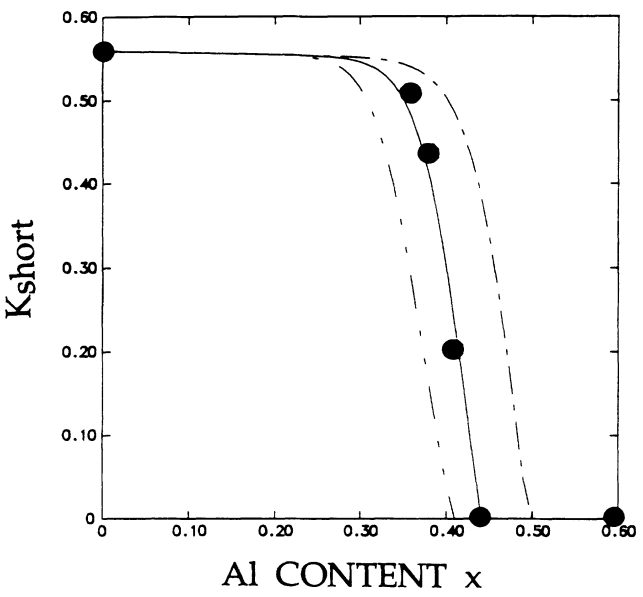

FIG. 3. K_{short} vs x. The solid curve shows the best fit of the calculated values of K_{short} from Eq. (2) to the experimental data (filled circles) with $\alpha=13.40$ meV/% and $x_c=0.412$. The dotted-dashed and double-dotted–dashed curves indicate the calculated values of K_{short} obtained by using the values (Ref. 19) of $\alpha=12.47$ meV/% and $x_c=0.45$, and that (Ref. 2) of $\alpha=14.55$ meV/% and $x_c=0.37$, respectively.

of α and x_c. The sensitivity in the determination of x_c by measuring K_{short} can be estimated by calculating the derivative dK_{short}/dx from Eq. (2). The value of dK_{short}/dx at $x=0.408$ was found to be 7.19, which means that if the value of x changes 0.01, the value of K_{short} will change 7.19% which is large enough to be measured. Since the relative standard probable error was ±0.07 for the experimental value of $K_{\text{short}}=0.193$ at $x=0.408$, the corresponding experimental uncertainty in x_c was determined to be ±0.002 from the relationship dK_{short}/dx.

The contribution of errors in the parameters used in fitting the data for the determination of x_c was also considered. For example, uncertainties in the previously measured intervalley and intravalley scattering times[11–13] of $t_{\Gamma X}=55\pm11$ fs, $t_{\Gamma L}=100\pm20$ fs, and $t_{\Gamma\Gamma}=165\pm20$ fs for GaAs could change the value of p_X for GaAs from 0.44 calculated using the maximum value of $t_{\Gamma X}=66$ fs and the minimum values of $t_{\Gamma L}=80$ fs and $t_{\Gamma\Gamma}=145$ fs, to 0.62 calculated using the minimum value of $t_{\Gamma X}=44$ fs, and the maximum values of $t_{\Gamma L}=120$ fs and $t_{\Gamma\Gamma}=185$ fs. This variation will affect the expression of the x dependence of $p_X(x)$ for $Al_xGa_{1-x}As$, and will change the determined value of x_c corresponding to the best fit. As mentioned above, based on the values of $t_{\Gamma X}=55$ fs, $t_{\Gamma L}=100$ fs, and $t_{\Gamma\Gamma}=165$ fs for GaAs, and the x dependence of the effective mass,[10] the deformation potential,[15] the alloy-disorder intervalley scattering,[16] and the energy gaps[10] for $Al_xGa_{1-x}As$, the fitting yielded $x_c=0.412$. However, the fitting gave a value of $x_c=0.417$ using one of the extreme set of values of $t_{\Gamma X}=66$ fs, $t_{\Gamma L}=80$ fs, and $t_{\Gamma\Gamma}=145$ fs for GaAs, and the corresponding x dependence of the parameters in Eqs. (2)–(4) for $Al_xGa_{1-x}As$, and a value of $x_c=0.407$ for the opposite extreme set of values of $t_{\Gamma X}=44$ fs, $t_{\Gamma L}=120$ fs, and $t_{\Gamma\Gamma}=185$ fs for GaAs, and the related x dependence for $Al_xGa_{1-x}As$. All other determined values of x_c from the fitting using other combinations of those measured values were found to fall in the range from 0.407 to 0.417. Therefore, the contribution of errors of the used intervalley and intravalley scattering times was determined to be ±0.005 for x_c. Similar analyses were done for errors in other parameters in Eqs. (2)–(4). The total contribution of errors in all the parameters used in the fitting was found to give an uncertainty in x_c of ±0.007.

In addition, the uncertainty in determining the Al content x for the samples was ±0.005. Consequently, the total uncertainty in x_c arising from the measurement for K_{short}, the determination of Al context x, and the errors of the parameters used for fitting was estimated to be $\pm\sqrt{0.002^2+0.005^2+0.007^2}=\pm0.009$.

For a comparison of our experimental results with the previously measured values of x_c, the calculated values of K_{short} as a function of x obtained by using the values[19] of $\Delta(E_g)^{\Gamma}/\Delta x=12.47$ meV/% and $x_c=0.45$, and that[2] of $\Delta(E_g)^{\Gamma}/\Delta x=14.55$ meV/% and $x_c=0.37$, are also displayed in Fig. 3. Our experimental data show that the critical value x_c is neither as large as 0.45 nor as small as 0.37, but 0.412.

In conclusion, the observed decay profiles of the induced IR absorption for $Al_xGa_{1-x}As$ reflect the type of band-structure gaps. From the change of K_{short}, with x, we have determined the values of $\Delta(E_g)^{\Gamma}/\Delta x=13.40$ meV/% and $x_c=0.412$ with a high degree of accuracy. Our measurement approach demonstrates the potential advantages of the femtosecond pump-IR-probe absorption technique to distinguish between direct and indirect band-gap structures for semiconductors. This method can be applied to search for useful direct band-gap alloys composed of indirect-gap elements, such as strained Ge/Si superlattice systems.

We would like to acknowledge Dr. N. Ockman for his helpful discussions. This research was supported in part by ARO and CUNY Organized Research.

[1]H. A. Zarem, J. A. Lebens, K. B. Nordstrom, P. C. Sercel, S. Sanders, L. E. Eng, A. Yariv, and K. J. Vahala, Appl. Phys. Lett. **55**, 2622 (1989).

[2]T. F. Kuech, D. J. Wolford, R. Potemski, J. A. Bradley, and K. H. Kelleher, Appl. Phys. Lett. **57**, 505 (1987).

[3]J. Shah, B. I. Miller, and A. E. DiGiovanni, J. Appl. Phys. **43**, 3434 (1972).

[4]E. E. Mendez, E. Calleja, and W. I. Wang, Phys. Rev. B **34**, 6026 (1986).

[5]W. W Ruhle, K. Leo, and E. Bauser, Phys. Rev. B **40**, 1756 (1989).

[6]H. J. Lee, L. Y. Juravel, and J. C. Woolley, Phys. Rev. B **21**,

659 (1980).
[7]W. B. Wang, Kai Shum, R. R. Alfano, D. Szmyd, and A. J. Nozik, Phys. Rev. Lett. **68**, 662 (1992).
[8]Kai Shum, W. B. Wang, R. R. Alfano, and K. M. Jones, Phys. Rev. Lett. **68**, 3904 (1992).
[9]W. B. Wang, N. Ockman, M. A. Cavicchia, and R. R. Alfano, Appl. Phys. Lett. **57**, 395 (1990).
[10]S. Adachi, J. Appl. Phys. **58**, R1 (1985).
[11]P. C. Becker, H. L. Fragnito, C. H. Brito Cruz, J. Shah, R. L. Fork, J. E. Cunningham, J. E. Henry, and C. V. Shank, Appl. Phys. Lett. **53**, 2089 (1988).
[12]J. Shah, B. Deveaud, T. C. Damen, W. T. Tsang, A. C. Gossard, and P. Lugli, Phys. Rev. Lett. **59**, 2222 (1987).
[13]J. A. Kash, J. C. Tsang, and J. M. Hvam, Phys. Rev. Lett. **54**, 2151 (1985).
[14]E. M. Conwell and M. O. Vassell, IEEE Trans. Electron. Devices **ED-13**, 22 (1966).
[15]S. Zollner, S. Gopalan, and M. Cardona, Appl. Phys. Lett. **54**, 614 (1989).
[16]H. Kalt, W. W. Ruhle, K. Reimann, M. Rinker, and E. Bauser, Phys. Rev. B **43**, 12 364 (1991).
[17]W. B. Wang, N. Ockman, M. Yan, and R. R. Alfano, J. Lumin. **50**, 347 (1992).
[18]B. Monemore, K. K. Shih, and G. D. Pettit, J. Appl. Phys. **47**, 2604 (1976).
[19]H. C. Casey, Jr., J. Appl. Phys. **49**, 3684 (1978).